OPEN

Chlorine as an Indicator in the Controllable Preparation of Active Nano-Gold Catalyst

Chengming Zhang[1,2], Lequan Liu[1], Xinjiang Cui[1], Lirong Zheng[3], Youquan Deng[1] & Feng Shi[1]

[1]Centre for Green Chemistry and Catalysis, Lanzhou Institute of Chemical Physics, Chinese Academy of Sciences, Lanzhou, 730000, China, [2]University of Chinese Academy of Sciences, Beijing, 100049, China, [3]Center for Multi-disciplinary Research, Institute of High Energy Physics, Chinese Academy of Sciences, Beijing, 100049, China.

The controllable preparation of nano-gold catalyst maintains a challenge. Except the parameters have been revealed before, here we'd like to show that controllable preparation of active nano-gold catalyst can be achieved using chlorine as an indicator. By tracing the chlorine concentration in the washing step, a series of Au/Fe$_2$O$_3$ catalysts were prepared with co-precipitation method. The applying of these catalysts in CO oxidation and reductive nitrobenzene N-alkylation suggested the active catalysts were prepared from solutions containing ~2 ppm chlorine. The catalytic activity dropped dramatically if the chlorine concentration is >4–6 or ≪1 ppm. Extensive characterizations revealed that the active catalyst was composed by nano-gold on the edge of Fe$_2$O$_3$ particle with 8.92 Au-Au coordination numbers. Although the real role of chlorine in the variation of catalyst structure and activity was still ambiguous, the current results should promote the controllable preparation of active nano-Au catalyst.

N ano-gold catalysis has received fantastic attentions since the discovery of the prominent behavior of nano-gold in CO low-temperature oxidation[1–5]. However, begin with the rising of nano-gold as a star in heterogeneous catalysis, the development of general rule to prepare active nano-gold catalyst, especially with co-precipitation method, is maintained as an unsolved problem till now. In order to find out the active site/ structure of nano-gold catalyst and thus to build a general methodology for nano-gold catalyst preparation, the relationship between the catalyst structure, which was produced through different preparation methods, and activity has been studied extensively. From the beginning of the study, it is revealed and well accepted that highly active nano-gold catalyst normally contains nano-gold particle with 2–4 nm size[6–8]. Then it is suggested that the interface between nano-Au particle and oxide support is the active centers[9]. Goodman and co-workers tried to connect the unusual catalytic activity with the quantum size effects of the very small gold particles and indeed they found the relationship[10]. They also showed that the bilayers of nano-gold were more active than the monolayers[11]. The role of cationic Au was also considered to be important in the generation of active site[12–18]. Possibly, cationic Au could form on the support surface and they contributed to the activity significantly, thus the presence of oxygen-rich surface should be important because it is helpful to produce Au$^{\sigma+}$[12,15]. Meanwhile, it was also reported that metallic Au was the active structure and oxidized Au was not necessary to achieve high activity[19]. Even the roles of supports were arguable. Although it has been studied extensively and was generally accepted that supports were crucial to obtain active nano-gold catalysts, some researchers tried to attribute the enhanced activity to the size effect alone[20–22]. The effect of pH value of aqueous solutions on the activity of nano-Au catalyst were also extensively studied and different rules were observed over different supports using deposition-precipitation method, which suggested that the speciation of gold prior to precipitation is important[23–27]. Apart from above results, one of the most acceptable operations to produce highly active nano-gold catalyst is the complete removal of chlorine[1,14–16,28–30] because we believe that the presence of chlorine is detrimental to gain active nano-gold catalysts.

In summary, the well accepted operations to prepare active nano-gold catalyst with co-precipitation method are as follows. 1) Choosing suitable catalyst precursors, i.e. chlorauric acid and transitional metal nitrate; 2) Choosing suitable bases, i.e. Na$_2$CO$_3$, K$_2$CO$_3$ and urea, etc; 3) Co-precipitation under suitable pH value, i.e. ~8–9, and completely removing of chlorine; 4) Aging the precipitate at suitable temperature, i.e. 80–120°C, and followed by calcination at ~350–400°C. Following the above operations, the active nano-gold catalyst usually composed by nano-gold with ~3 nm particle size deposited on the edge of metal oxide supports. Fairly controlling of the

above operations is essential to gain active nano-gold catalyst with suitable sizes of gold and support, and suitable electronic interaction between nano-gold particle and support through generating fine structure of gold-support interface.

However, the controllable preparation of active nano-gold catalyst is still difficult even if we know the important parameters to gain active nano-gold catalyst as discussed above. During our long-time work on the controllable preparation of active nano-gold catalyst, we found that one simple but important parameter was neglected during the catalyst preparation, i.e. accurate controlling of chlorine concentration, due to the using of $AgNO_3$ as detecting agent. The fatal aspect is its test limit, i.e. in aqueous solution, it is ~6 ppm determined by potentialstatic scanning with electrochemical station[31]. Thus, we can't control the washing step when the chlorine concentration is lower than 6 ppm. In another word, we can't relate the catalytic activity with the chlorine concentration when it is < 6 ppm. In the past 20 years, this simple but pivotal point was neglected because chlorine was always considered to be poisonous to active nano-gold catalyst. Possibly, the variation of chlorine concentration caused the un-reproducibility of nano-gold catalyst.

Here we'd like to present our new results about the controllable preparation of nano-gold catalyst by fine tracing the chlorine concentration of the aqueous solution, which contains the precipitated catalyst precursors, in the range of 0 to hundred ppm, in the washing step. A classical supported nano-Au catalyst for CO oxidation, i.e. Au/Fe_2O_3, was used as the model catalyst which also received extensive attentions in the last years[32–37]. For this catalyst, the iron oxide is one of the most effective supports for nano-gold catalyst and it is also very sensitive to the preparation procedure[38]. The co-precipitation method was chosen for catalyst preparation because it often results in reproducibility problem, too. We hope the controllable preparation of active nano-gold catalyst can be realized if we follow the classical operations as discussed above and meanwhile trace the concentrations of chlorine during catalyst preparation.

Results

Initially, the catalytic activities of 8 Au/Fe_2O_3-X samples were tested carbon monoxide oxidation reaction. These catalysts were prepared from aqueous solutions with chlorine concentrations in the range of 0 to 110 ppm determined by potentialstatic scanning with electrochemical station. According to the results shown in Fig. 1, clearly,
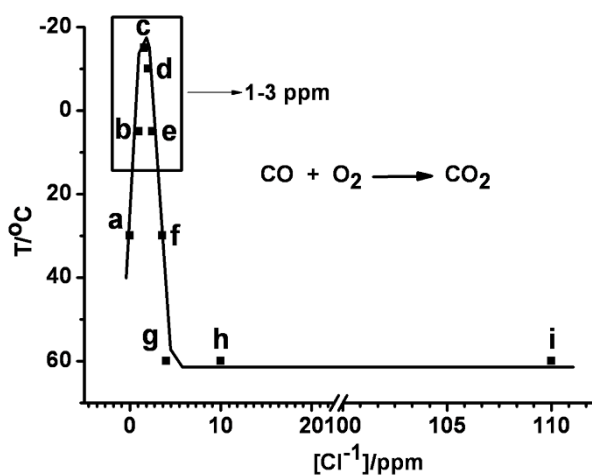
there is a peak area in catalytic activity, i.e. catalyst samples prepared from 1–3 ppm chlorine concentration possessed the best activity. The highest activities were obtained with catalysts Au/Fe_2O_3-0.19, with which the CO oxidation temperature was <−10°C. Furthermore, there are two boundaries of the dramatic decrease in catalytic activity. One point is 1.0 ppm, the other point is ~3–4 ppm. It is easy to understand the lower catalytic activity when the chlorine concentration is higher than 3–4 ppm because it is well known that the presence of chlorine would deactivate the catalyst. However, the remarkable dropping in catalytic activity is very strange if further remove chlorine when its concentration in aqueous solution is close to 1 ppm. As it was shown in the experimental section, the only difference in these samples was that they were prepared from aqueous solutions with different chlorine concentrations. It is really difficult to explain these strange results. Further on, the steady-state CO oxidation rate of catalysts Au/Fe_2O_3-0.18, Au/Fe_2O_3-0.19 and Au/Fe_2O_3-0.21 were measured in a fixed-bed reactor at atmospheric pressure. The CO conversions over these three catalysts were 4.6%, 5.5% and 6.8% after changing the catalyst loadings and space velocity. Clearly, the CO oxidation rates over catalysts Au/Fe_2O_3-0.18 and Au/Fe_2O_3-0.21 were 0.236–0.237 mol_{CO}/mol_{Au}/min. Much higher oxidation rate was observed over Au/Fe_2O_3-0.19. It was 1.154 mol_{CO}/mol_{Au}/min. This number is almost 5 times higher than those obtained with Au/Fe_2O_3-0.18 and Au/Fe_2O_3-0.21.

Although the rule about the relationship of chlorine concentration with the activity of final catalyst was inspirable using carbon monoxide oxidation as model reaction, it should be interesting to check its universality in other reactions. However, as it is well accepted, the suitable preparation method and condition is specific for one particular catalyst, some time it is specific for one particular reaction, to gain high activity especially in nano-Au catalysis. Normally, the preparation method and condition need to be tuned again even the same catalyst is employed if the reaction is changed. Therefore, in order to exclude the unexpected influencing factors as far as possible, the coupling reaction of nitrobenzene and benzyl alcohol, Fig. 2, which has been shown that Au/Fe_2O_3 was active catalyst in our laboratory[31], was selected to check the universality of our observation. By tracing the catalytic activity of 30 Au/Fe_2O_3 catalyst samples prepared from aqueous solutions with 0–390 ppm chlorine, clearly, there is also a peak area in the catalytic activity, i.e. catalyst samples prepared from 1–4 ppm chlorine concentration possessed the best activity, which normally produced 80–88% yields to N-benzyl aniline. Furthermore, there are two boundaries of the dramatic decrease in catalytic activity. One point is 4–5 ppm, the other point is ~1 ppm. Although the chlorine concentration field is slightly wider than that observed in carbon monoxide oxidation, the same rule was obtained.

Figure 1 | **The total oxidation temperature of carbon monoxide vs the chlorine concentration of the aqueous solution from which the catalyst samples were prepared.** (a) ≪ 1 ppm; (b) 1.0 ppm; (c) 1.6 ppm; (d) 2.0 ppm; (e) 2.5 ppm; (f) 3.6 ppm; (g) 4.0 ppm; (h) 10.0 ppm and (i) 110 ppm. The carbon monoxide conversions at (g), (h) and (i) were all < 5%.
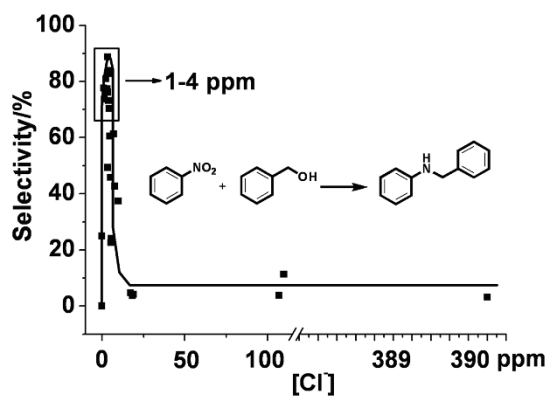

Figure 2 | **The selectivity to N-benzyl aniline *vs* the chlorine concentration of the aqueous solution from which the catalyst samples were prepared.**

Discussion

In order to find out what caused this significant difference in catalytic activity, four typical samples, i.e. Au/Fe_2O_3-0.18, Au/Fe_2O_3-0.19, Au/Fe_2O_3-0.21 and Au/Fe_2O_3-0.72, were characterized by ICP, XPS and BET. The data were given in Table 1 and the typical XPS spectra were shown in Fig. S1. Clearly, the Au loadings are similar in these samples. Interestingly, the chlorine loadings on Au/Fe_2O_3-0.18, Au/Fe_2O_3-0.19 and Au/Fe_2O_3-0.21 were very similar although the chlorine concentrations in the aqueous solutions at the final step of washing were different. It is difficult to explain it at this stage. Possibly, small amounts of chlorine can be attached onto the catalysts relatively stable and is difficult to be washed away. The relationship between BET surface areas of the catalyst samples and chlorine concentrations was also interesting. By comparing the composition of the most active Au/Fe_2O_3-0.19 with other samples, it can be seen clearly that it has the highest BET surface area, i.e. 103 m^2/g, whereas the surface area decreased no matter it is prepared from aqueous solutions with higher or lower chlorine concentrations. The large variation of surface areas might be derived from the presence of different amounts of chlorine and also possibly caused by the washing operation. But it is difficult to determine the major factor currently. Furthermore, the binding energies of Au species in different samples were also dropped in the same scope, i.e. 84.0 ± 0.1 eV. These results suggested the formation of metallic gold species in these samples. If we consider the results of catalytic reaction together with the characterization, it can be concluded partially that the formation of iron oxide supports with different properties is one of the possible reasons to produce catalysts with different catalytic activities, which would result in significant changes in gold-oxide interactions and consequently the catalytic properties.

Then, five typical samples including Au/Fe_2O_3-0.18, Au/Fe_2O_3-0.19, Au/Fe_2O_3-0.21, Au/Fe_2O_3-0.27 and Au/Fe_2O_3-0.72 were characterized by XRD, Fig. S2, the typical diffraction patterns of α-Fe_2O_3 were observed in all the samples. What interesting is that the intensity of the XRD diffraction patterns of sample Au/Fe_2O_3-0.19 is weaker than other samples. All the catalysts prepared from aqueous solutions with higher chlorine concentrations or with lower chlorine concentrations generated better crystallized iron oxide. Similar phenomena were observed from the diffraction patterns of gold but only Au (111) appeared except sample Au/Fe_2O_3-0.19, from which there is no observable gold diffraction pattern. These results suggested the formation of highly dispersed nano-gold on less crystallized iron oxide in sample Au/Fe_2O_3-0.19. These results can explain the better catalytic performance of Au/Fe_2O_3-0.19 in the CO oxidation reaction, i.e. formation of small nano-Au particle on less crystallized iron oxide.

According to the TEM measurement, more information was obtained, Fig. 3. First, the particle sizes of samples Au/Fe_2O_3-0.18, Au/Fe_2O_3-0.19 and Au/Fe_2O_3-0.21 were all ~3 nm, which was dropped in the commonly accepted area of nano-gold with high activity, i.e. 2–4 nm[6–8]. For sample Au/Fe_2O_3-0.27, the nano-gold particle size is >6 nm. It confirmed the observation from XRD characterization and also the reason for its low activity. In Au/Fe_2O_3-0.18, the nano-gold particle was deposited on the plain of iron oxide. The crystal lattices of Au (111) and Fe_2O_3 (104) are distinct and without strong interaction with each other. In sample Au/Fe_2O_3-0.19, many observable nano-gold particles were deposited on the edge of iron oxide particles, and distinct interface between nano-gold and iron oxide formed. In consideration of the best catalytic performance of this sample, the observation strongly supports the former results about active site in nano-gold catalyst, i.e. the interface between nano-gold and iron oxide[9]. For samples prepared from aqueous solutions with higher chlorine concentrations, i.e. Au/Fe_2O_3-0.21, it can be seen that the nano-gold particles moved from the edge of iron oxide into the plain and stronger interaction occurred between gold particle and iron oxide, in which their crystal lattices were overlapped with each other and the gold particle was surrounded with well crystallized iron oxide. This could be clearer from the results of Au/Fe_2O_3-0.27. In this sample, the nano-gold species were possibly wrapped inside the Fe_2O_3 and bigger gold particle is forming from several smaller gold particles. This is easily acceptable and there is no any argument because the presence of large amounts of chlorine will cause gold particle coagulation[1,14,16,28–30,39]. Thus, according to the discussions above, we can suppose that an active nano-gold catalyst with nano-gold deposited on the edge of iron oxide particle can be prepared from solutions containing ~2 ppm chlorine. If the chlorine is further removed, the nano-Au particle would move to the iron oxide plane during washing but coagulation of nano-Au particle occurred if too much chlorine is presented, i.e. > 4 ppm.

Although only α-Fe_2O_3 and weak diffraction patterns of Au (111) were observed by XRD characterization, we tried to get more information about the effect of chlorine concentrations on the structure of Fe_2O_3 support. Therefore, Mössbauer spectra of Au/Fe_2O_3-0.18, Au/Fe_2O_3-0.19, Au/Fe_2O_3-0.21 and Au/Fe_2O_3-0.72 were recorded at room temperature. The Mössbauer spectra were shown in Fig. 4 and the characterization parameters were listed in Table S1. The spectra of Au/Fe_2O_3-0.18 can be fitted to one sextet with IS = 0.37 mm/s and QS = −0.11 mm/s, which was assigned to α-Fe_2O_3 (A)[40], Fig. 4(a). The spectra of Au/Fe_2O_3-0.19 and Au/Fe_2O_3-0.21 can be fitted to two sextets and one doublet, Fig. 4(b) and (c). The outer sextets with IS of 0.37 and 0.41 mm/s, and QS of −0.11 and −0.24 mm/s were assigned to α-Fe_2O_3 (A)[40]. The inner sextets with IS of 0.39 and 0.40 mm/s, and QS of −0.09 and −0.24 mm/s was associated to α-Fe_2O_3 (B) but it was not conclusive[41]. The strange point for sample Au/Fe_2O_3-0.19 and Au/Fe_2O_3-0.21 were the doublet peaks with IS = 0.37/0.33 mm/s and QS = 0.80/0.78 mm/s. This might be for the high-spin Fe^{3+} in an octahedral oxygen environment[42]. The IS and QS values are consistent with super-paramagnetic behavior identified in Mössbauer measurements of nano-sized α-Fe_2O_3 with a particle size below 8 nm[42,43]. Thus, 17.8% and 8.5% nano-sized α-Fe_2O_3 was possibly formed inside the bulk α-Fe_2O_3 with particle size smaller than 8 nm in samples Au/Fe_2O_3-0.19 and Au/Fe_2O_3-0.21. For Au/Fe_2O_3-0.72, the raw spectra can be fitted to two sextets, Fig. 4(d). These were similar as those observed from Au/Fe_2O_3-0.19, i.e. α-Fe_2O_3 (A) and (B). These results suggested that the slight changing of chlorine concentration in aqueous solution, from which the catalysts were prepared, influenced the structure of Fe_2O_3 remarkably. With regarding to the catalytic activity, if it is related to the composition of the Fe_2O_3, it can be imagined that the formation of nano-α-Fe_2O_3 is helpful to build the active sites. Higher catalytic activity was obtained with the formation of more nano-α-Fe_2O_3 if comparing the catalytic performance of Au/Fe_2O_3-0.19 and Au/Fe_2O_3-0.21.

Following, we tried to study the variation of catalyst structures with chlorine concentrations by EXAFS characterization, Fig. 5. According to the radial distribution functions obtained by Fourier

Table 1 | Physicochemical properties of typical Au/Fe_2O_3 catalyst samples

Entry	Catalysts	Au/wt%[a]	[Cl^-]/wt%[b]	$Au_{4f7/2}$ (eV)[c]	S_{BET}/ m^2/g
1	Au/Fe_2O_3-0.18[d]	2.82	0.18	84.1	57
2	Au/Fe_2O_3-0.19	2.94	0.19	84.0	103
3	Au/Fe_2O_3-0.21	3.19	0.21	84.0	66
4	Au/Fe_2O_3-0.72	2.77	0.72	84.0	24

[a]Determined by ICP measurement.
[b]Determined by potentialstatic-scanning method with a CHI660D electrochemical workstation by dissolving quantitative amount of catalyst sample in dilute nitric acid.
[c]Determined by XPS.
[d]During the preparation of this sample, the chlorine concentration can not be tested accurately but far below 1 ppm as described in experimental section.
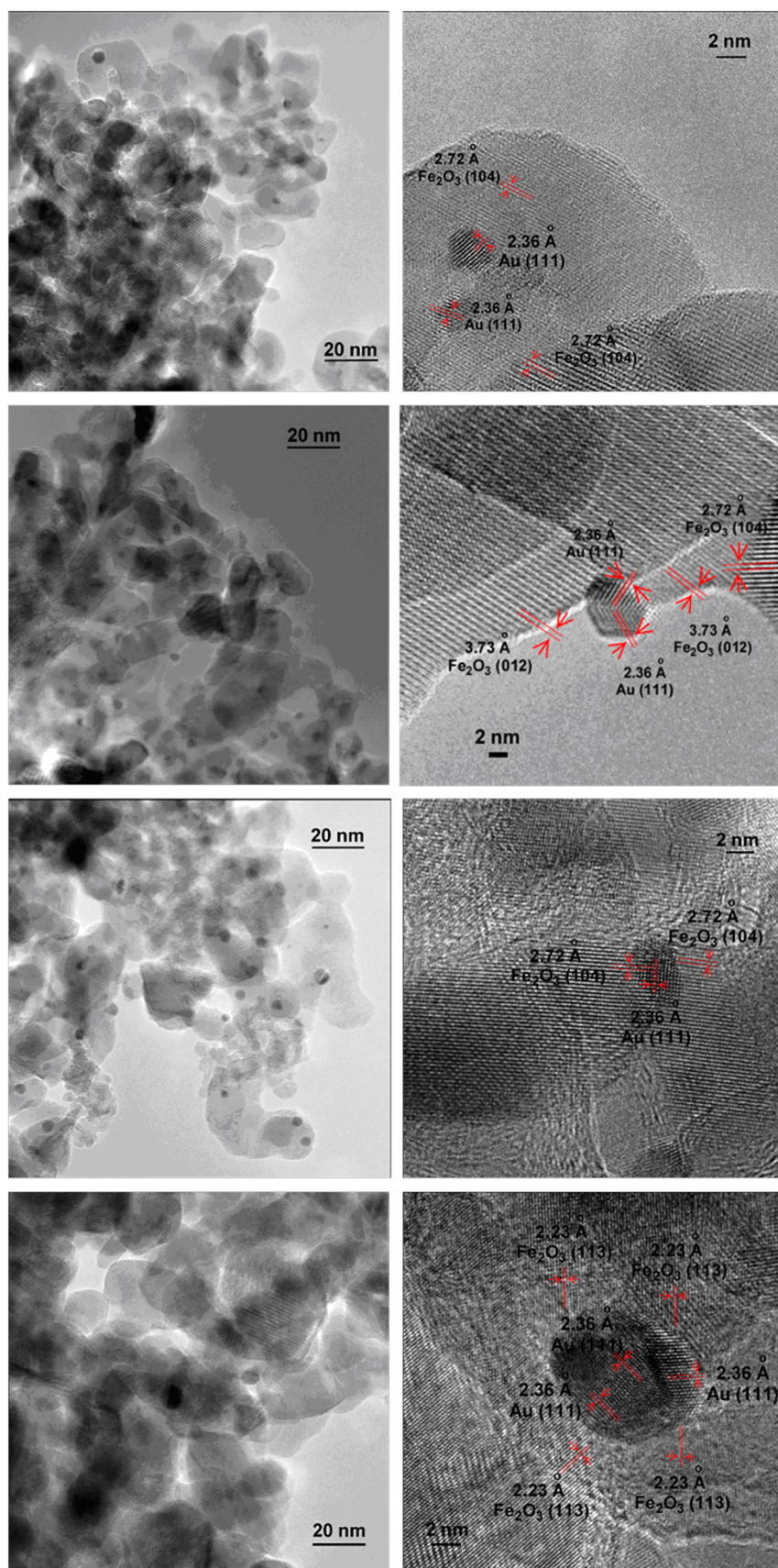
Figure 3 | TEM pictures of Au/Fe$_2$O$_3$-0.18, Au/Fe$_2$O$_3$-0.19, Au/Fe$_2$O$_3$-0.21 and Au/Fe$_2$O$_3$-0.72 (from upside).
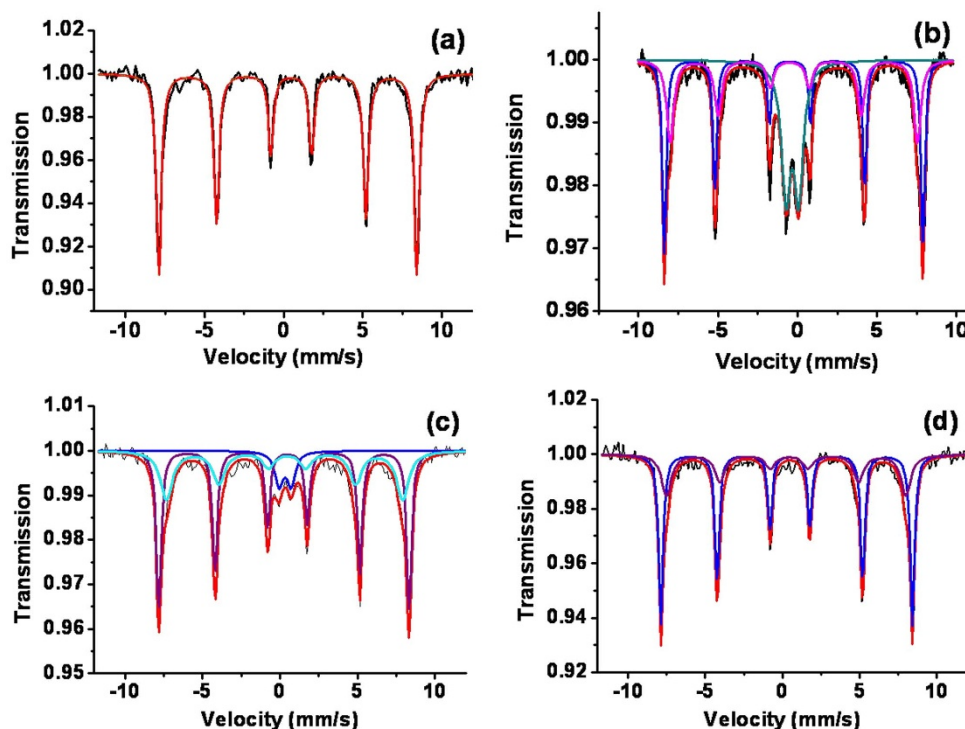
Figure 4 | Mössbauer spectra of (a) Au/Fe$_2$O$_3$-0.18, (b) Au/Fe$_2$O$_3$-0.19, (c) Au/Fe$_2$O$_3$-0.21 and (d) Au/Fe$_2$O$_3$-0.72 at room temperature.

Transformation (FT), similar EXAFS spectra were obtained from samples Au/Fe$_2$O$_3$-0.18, Au/Fe$_2$O$_3$-0.19 and Au/Fe$_2$O$_3$-0.21. If we compare their spectra with the spectra of standard samples of gold foil, gold oxide and gold chloride, it can be seen that there is no Au-Cl in all the samples! Moreover, the spectra of the catalyst samples are almost the same as the gold foil, which suggests the major gold species are metallic gold and confirms the results of XPS characterization. Further analysis of the EXAFS data suggested that only Au-Au coordination was observed and the results were given in Table 2. The Au-Au coordination numbers in samples Au/Fe$_2$O$_3$-0.18, Au/Fe$_2$O$_3$-0.19 and Au/Fe$_2$O$_3$-0.21 were 8.64, 8.92 and 9.21, respectively. That means with the increasing of the chlorine concentration, the coordination numbers of Au-Au increased, which is finally close to the coordination number of pure Au foil. Possibly, 8.92 is the suitable coordination number of Au-Au to exhibit high catalytic activity.
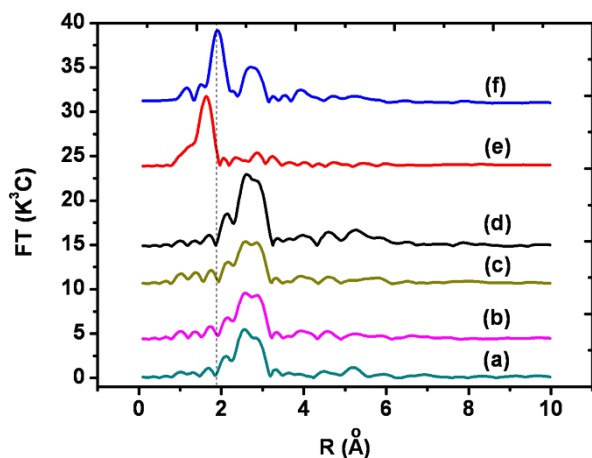
Based on the reaction and characterization results discussed above, the relationship among catalyst structure, catalytic activity and chlorine concentrations of the aqueous solutions has been clarified. Although it is difficult to discover the real role of chlorine now, the controllable preparation of active nano-gold by tracing chlorine concentrations can be realized. The procedure for active nano-gold catalyst preparation was illustrated in Fig. 6 using Au/Fe$_2$O$_3$ as model catalyst and co-precipitation as model method. It must be mentioned that the first step for active nano-gold catalyst preparation by tracing chlorine concentration should be the determination of other essential parameters, i.e. catalyst precursors, base, pH value for co-precipitation, calcination temperature, etc.

In conclusion, following the known essential operations and tracing the chlorine concentrations finely, the controllable preparation of active nano-gold catalyst was realized and active nano-gold catalyst can be obtained when the chlorine concentration dropped in the range of 1–4 ppm. The major special structure of the active nano-gold catalyst is ~3 nm nano-gold deposited on the edge of iron oxide particle with 8.92 Au-Au coordination numbers. This is the first time to show that the washing step for chlorine removing should be controlled when it is <6 ppm because the nano-Au catalyst turns inactive if the chlorine concentration in the aqueous solution is far below 1 ppm.

Figure 5 | Fourier transform (FT) of Au L$_{III}$-edge EXAFS for (a) Au/Fe$_2$O$_3$-0.18, (b) Au/Fe$_2$O$_3$-0.19, (c) Au/Fe$_2$O$_3$-0.21, (d) gold foil, (e) Au$_2$O$_3$ and (f) AuCl$_3$.

Table 2	EXAFS Fitting Parameters at the Au$_{LIII}$-Edge[a]				
Samples	Shell	N	R$_i$ (Å)	σ² (Å²)	ΔE$_0$ (eV)
Au/Fe$_2$O$_3$-0.18	Au-Au	8.64	2.85	0.659	4.95
Au/Fe$_2$O$_3$-0.19	Au-Au	8.92	2.85	0.645	5.23
Au/Fe$_2$O$_3$-0.21	Au-Au	9.21	2.84	0.638	4.48
Au Foil	Au-Au	9.94	2.86	0.805	4.44

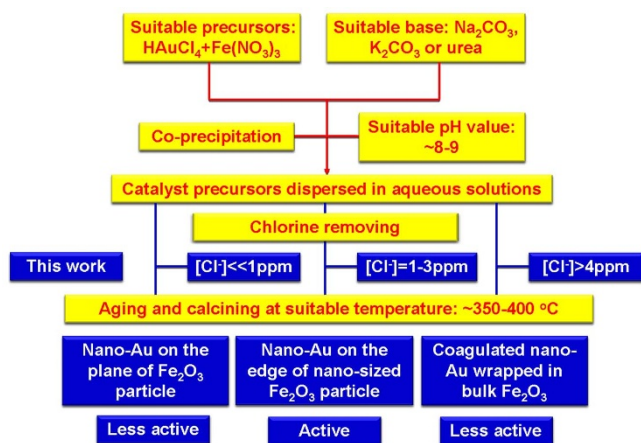[a]N, coordination number; R$_i$, bonding distance; σ², Debye-Waller factor; ΔE$_0$, inner potential shift.

Figure 6 | An illustration for the chlorine concentration mediated preparation of active Au/Fe₂O₃ catalyst with co-precipitated method. Yellow: Known parameters for active nano-Au catalyst preparation; Blue: New parameters revealed in our work.

Methods

General. All solvent and chemicals were obtained commercially and were used as received. High-resolution TEM analysis was carried out on a Tecnai-G2-F30 field emission transmission electron microscope. The catalyst samples after pretreatment were dispersed in ethanol, and the solution was mixed ultrasonically at room temperature. A part of solution was dropped on the grid for the measurement of TEM images. XRD measurements are conducted by an X'Pert PRO (PANalytical) diffractometer. The XRD diffraction patterns were scanned in the 2θ range of 10–80°. X-ray photoelectron spectroscopy (XPS) analysis was measured using a K-Alpha-surface analysis instrument with Al Kα radiation (1361 eV). Nitrogen adsorption-desorption isotherms were measured at 77 K using Micromeritics 2010 instrument. The pore-size distribution was calculated by Barrett, Joyner and Halenda (BJH) method from desorption isotherm. The Au content of the catalysts was measured by inductively coupled plasma-atomic emission spectrometry (ICP-AES), using an Iris advantage Thermo Jarrel Ash device. The Mössbauer spectra were obtained at room temperature with a Wissel electromechanical spectrometer (Wissenschaftliche Elektronik GmbH, Germany) working in a constant acceleration mode. A ^{57}Co/Pd (activity $\cong$ 25 m Ci) source and α-Fe standard were used. The experimentally obtained spectra were fitted to mathematical processing according to the least squares method. The parameters of hyperfine interaction such as isomer shift (IS), quadrupole splitting (QS), hyperfine magnetic field (H_{hf}), and the relative area of the partial components in the spectra were determined. Extended X-ray ab-sorption fine structure (EXAFS) experiments were performed at the Beijing Synchrotron Radiation Facility (BSRF), Beijing Institute of High Energy Physics, Chinese Academy of Sciences with storage ring energy of 2.5 GeV and a beam current between 150 and 250 mA. The Au L_{III} edge absorbance of powder catalysts was measured in transmission geometry at room temperature. The energy was scanned from −200 eV below to 1000 eV above the Au L_{III} edge (11919 eV). EXAFS data analysis was carried out using iffeffit analysis programs (http://cars9.uchicago.edu/ifeffit/). Radial distribution functions were ob-tained by Fourier-transformed k3-weighted χ function. The Cl⁻ ion concentration was tested at 25.0°C through potentialstatic scanning on a CHI660D electrochemical workstation. A Cl⁻ ion electrode was used as a working electrode and a platinum wire and an Ag/AgCl electrode were used as counter and reference electrodes respectively. Before analysis, a series of Cl⁻ ion standard solutions including 2.0 ppm, 4.0 ppm, 8.0 ppm, 40.0 ppm, 200.0 ppm and 400.0 ppm were prepared using NaCl as the Cl⁻ ion source. The potentialstatic scanning was carried out at interval of 0.1 s for 1 min in the standard solutions, and the corresponding average potential value (mV) was obtained, which were repeated three times. The electrode system was calibrated with a 5.0 ppm standard solution and the chlorine determination could be carried out through potentialstatic scanning when it is in the range of 5.0 ± 0.5 ppm. The test limit about this method is ~1 ppm.

Au/Fe₂O₃ catalyst preparation. Aqueous solutions (20 mL) of Fe(NO₃)₃·9H₂O (13.0 mmol, 5.24 g) and HAuCl₄ (1.05 mL, 1 g/10 mL H₂O) were mixed and added into 75 mL Na₂CO₃ solution (0.47 M) under vigorous stirring in 0.5 h. It was further stirred for 0.5 h, ultrasonically washed for 1 h and ~110 mL turbid liquid was obtained. Then ~36 mL turbid liquid was taken out under vigorous stirring and centrifuged (5000 rpm for 10–20 min). The recovered precipitate was re-dispersed in 200 mL deionized water and further ultrasonically washed for 1 h to remove chlorine. In the end of the operation, the chlorine concentration in aqueous solution was 3~4 ppm determined by potentialstatic scanning method with a CHI660D electrochemical workstation. Then the resulting slurries was heated up to 350°C in 0.5 h under air flow (2 mL/S) and maintained for 5 h. By varying the amounts of water added in the final step, a series of samples prepared from aqueous solutions with

different chlorine concentrations were obtained. The sample was denoted as Au/Fe₂O₃-X, in which X suggested the residual chlorine in the catalysts in ppm. Here, five typical catalyst samples were characterized systematically, i.e. Au/Fe₂O₃-0.18, Au/Fe₂O₃-0.19, Au/Fe₂O₃-0.21, Au/Fe₂O₃-0.27 and Au/Fe₂O₃-0.72, which were prepared from aqueous solutions containing 0, 1.6, 4.1, 10.0 and 110 ppm chlorine. For sample Au/Fe₂O₃-0.18, ~55 mL turbid liquid was taken out from the first step under vigorous stirring and centrifuged (5000 rpm for 10–20 min). The recovered precipitate was re-dispersed in 1000 mL deionized water and further ultrasonically washed for 0.5 h to remove chlorine. The operation was repeated for 4 times and the resulted solid was treated under the same conditions as above. According to the potentialstatic scanning measurement, the chlorine concentration in the final step is $\ll$ 1 ppm. For the purpose of getting comparable results, all the batches were performed under strictly controlled conditions and the only difference in all the catalyst samples was the chlorine concentration in aqueous solutions before catalyst precursor separation, drying and calcination. In order to show the generality of our observation, two different reactions were used here for activity measurement. The first one is the classical low-temperature CO oxidation and another one is the reductive coupling of nitrobenzene and benzylalcohol[31,44,45].

Reaction conditions for the low-temperature CO oxidation. CO oxidation activity measurements were carried out in a fixed-bed reactor at atmospheric pressure with 80 mg of catalyst. The feed gas for the oxidation was about 1 vol% CO balanced with air (without further purification). The space velocity of the measurement was 11000 mL·g⁻¹·h⁻¹. The concentrations of CO and O₂ in the effluent gas were analyzed on-line by a gas chromatograph equipped with a thermal conductivity detector (TCD) using Ar as carrier gas. The conversion of CO was calculated from the change in CO concentration between the inlet and outlet gases with a thermal conductivity detector (TCD).

Reaction conditions for the coupling of nitrobenzene and benzyl alcohol. 5.0 mmol (615 mg) nitrobenzene, 50.0 mmol (5400 mg) benzyl alcohol and 100 mg Au/Fe₂O₃ were added into a 25 mL pressure tube. Then, it was reacted at 180°C (oven temperature) under argon atmosphere for 1 h. After it was cooled to room temperature, the reaction mixture was dissolved in acetone and analyzed by GC-MS (Agilent 6890/5973). 30 catalyst samples prepared parallel from several batches. The conversions were all > 99% and the major byproduct in the reaction is N-benzylideneaniline.

Steady-state CO oxidation rate measurements. CO oxidation rates were measured in a fixed-bed reactor at atmospheric pressure. CO conversions were kept ~5% by changing the catalyst loadings and space velocity while keeping the temperature at 298 K. These low conversions ensure the differential nature of measured rates and avoid their rigorous but more cumbersome interpretation in terms of integral equations. In this work, typically, catalysts Au/Fe₂O₃-0.18, Au/Fe₂O₃-0.19 and Au/Fe₂O₃-0.21 (10.0, 6.0 and 20.0 mg, respectively) were diluted with aluminum oxide (100 mg). The catalyst samples were treated and stabilized in flowing 1 vol% CO (balanced with air, 18.0 mL/min, 45.9 mL/min and 27.5 mL/min, respectively) at 298 K for 1 h. Then, the CO conversions were measured at 298 K. The CO conversions over Au/Fe₂O₃-0.18, Au/Fe₂O₃-0.19 and Au/Fe₂O₃-0.21 were 4.6%, 5.5% and 6.8%, respectively.

The CO oxidation rates were calibrated according to the following formula.

$$R_{CO}(mol_{CO}/mol_{Au}\cdot min) = M_{CO}/Cat._m \times Au\ wt\% / 197$$

$$M_{CO} = V \times 0.01 \times Con._{CO} \times P/R \times 298$$

R_{CO}: CO oxidation rate; M_{CO}: mol of CO converted in 1 min; $Cat._m$: Catalyst loading; Au wt%: Au loading in the catalyst sample; V: total volume of 1 vol% CO passed the catalyst per minute.

1. Haruta, M., Yamada, N., Kobayashi, T. & Iijima, S. Gold catalysts prepared by coprecipitation for low-temperature oxidation of hydrogen and of carbon-monoxide. *J. Catal.* **115**, 301–309 (1989).
2. Hashmi, A. S. K. & Hutchings, G. J. Gold catalysis. *Angew. Chem. Int. Ed.* **45**, 7896–7936 (2006).
3. Min, B. K. & Friend, C. M. Heterogeneous gold-based catalysis for green chemistry: Low-temperature CO oxidation and propene oxidation. *Chem. Rev.* **107**, 2709–2724 (2007).
4. Corma, A. & Garcia, H. Supported gold nanoparticles as catalysts for organic reactions. *Chem. Soc. Rev.* **37**, 2096–2126 (2008).
5. Gong, J. L. & Mullins, C. B. Surface science Iinvestigations of oxidative chemistry on gold. *Acc. Chem. Res.* **42**, 1063–1073 (2009).
6. Valden, M., Pak, S., Lai, X. & Goodman, D. W. Structure sensitivity of CO oxidation over model Au/TiO₂ catalysts. *Catal. Lett.* **56**, 7–10 (1998).
7. Choudhary, T. V. & Goodman, D. W. Oxidation catalysis by supported gold nano-clusters. *Top. Catal.* **21**, 25–34 (2002).
8. Haruta, M. *et al.* Low-temperature oxidation of Co over gold supported on TiO₂, alpha-Fe₂O₃, and Co₃O₄. *J. Catal.* **144**, 175–192 (1993).
9. Bond, G. C. & Thompson, D. T. Gold-catalysed oxidation of carbon monoxide. *Gold Bull.* **33**, 41–51 (2000).

10. Valden, M., Lai, X. & Goodman, D. W. Onset of catalytic activity of gold clusters on titania with the appearance of nonmetallic properties. *Science* 281, 1647–1650 (1998).

11. Chen, M. S. & Goodman, D. W. The structure of catalytically active gold on titania. *Science* 306, 252–255 (2004).

12. Sinha, A. K., Seelan, S., Tsubota, S. & Haruta, M. A three-dimensional mesoporous titanosilicate support for gold nanoparticles: Vapor-phase epoxidation of propene with high conversion. *Angew. Chem. Int. Ed.* 43, 1546–1548 (2004).

13. Finch, R. M. *et al.* Identification of active phases in Au-Fe catalysts for low-temperature CO oxidation. *Phys. Chem. Chem. Phys.* 1, 485–489 (1999).

14. Golunski, S., Rajaram, R., Hodge, N., Hutchings, G. J. & Kiely, C. J. Low-temperature redox activity in co-precipitated catalysts: a comparison between gold and platinum-group metals. *Catal. Today* 72, 107–113 (2002).

15. Lee, S. J. & Gavriilidis, A. Supported Au catalysts for low-temperature CO oxidation prepared by impregnation (vol 206, pg 305, 2002). *J. Catal.* 211, 283–283 (2002).

16. Guzman, J. & Gates, B. C. Structure and reactivity of a mononuclear gold-complex catalyst supported on magnesium oxide. *Angew. Chem. Int. Ed.* 42, 690–693 (2003).

17. Guzman, J. & Gates, B. C. A mononuclear gold complex catalyst supported on MgO: spectroscopic characterization during ethylene hydrogenation catalysis. *J. Catal.* 226, 111–119 (2004).

18. Hutchings, G. J. *et al.* Role of gold cations in the oxidation of carbon monoxide catalyzed by iron oxide-supported gold. *J. Catal.* 242, 71–81 (2006).

19. Fan, L., Ichikuni, N., Shimazu, S. & Uematsu, T. Preparation of Au/TiO$_2$ catalysts by suspension spray reaction method and their catalytic property for CO oxidation. *Appl. Catal. A: Chem.* 246, 87–95 (2003).

20. Davis, R. J. All that glitters is not Au-0. *Science* 301, 926–927 (2003).

21. Schwartz, V. *et al.* XAS study of Au supported on TiO$_2$: Influence of oxidation state and particle size on catalytic activity. *J. Phys. Chem. B* 108, 15782–15790 (2004).

22. Yang, J. H. *et al.* Activation of Au/TiO$_2$ catalyst for CO oxidation. *J. Phys. Chem. B* 109, 10319–10326 (2005).

23. Lee, S. J. & Gavriilidis, A. Supported Au catalysts for low-temperature CO oxidation prepared by impregnation. *J. Catal.* 206, 305–313 (2002).

24. Chang, C. K., Chen, Y. J. & Yeh, C. T. Characterizations of alumina-supported gold with temperature-programmed reduction. *Appl. Catal., A: Chem.* 174, 13–23 (1998).

25. Wolf, A. & Schuth, F. A systematic study of the synthesis conditions for the preparation of highly active gold catalysts. *Appl. Catal., A: Chem.* 226, 1–13 (2002).

26. Moreau, F. & Bond, G. C. Gold on titania catalysts, influence of some physicochemical parameters on the activity and stability for the oxidation of carbon monoxide. *Appl. Catal. A: Chem.* 302, 110–117 (2006).

27. Tsubota, S., Cunningham, D. A. H., Bando, Y. & Haruta, M. Preparation of nanometer gold strongly interacted with TiO$_2$ and the structure sensitivity in low-temperature oxidation of CO. *Stud. Surf. Sci. Catal.* 91, 227–235 (1995).

28. Hugon, A., El Kolli, N. & Louis, C. Advances in the preparation of supported gold catalysts: Mechanism of deposition, simplification of the procedures and relevance of the elimination of chlorine. *J. Catal.* 274, 239–250 (2010).

29. Bond, G. C., Louis, C. & Thompson, D. T. In *Catalytic Science Series* Vol. 6, (ed Hutchings, G. J.) 89 (Imperial College Press, Singapore, 2006).

30. Louis, C. Vol. 1, (ed Astruc, D.) 478 (Wiley-VCH, Weinheim, 2008).

31. Peng, Q. L., Zhang, Y., Shi, F. & Deng, Y. Q. Fe$_2$O$_3$-supported nano-gold catalyzed one-pot synthesis of N-alkylated anilines from nitroarenes and alcohols. *Chem. Commun.* 47, 6476–6478 (2011).

32. Shodiya, T., Schmidt, O., Peng, W. & Hotz, N. Novel nano-scale Au/α-Fe$_2$O$_3$ catalyst for the preferential oxidation of CO in biofuel reformate gas. *J. Catal.* 300, 63–69 (2013).

33. Li, L. *et al.* Origin of the high activity of Au/FeO$_x$ for low-temperature CO oxidation: Direct evidence for a redox mechanism. *J. Catal.* 299, 90–100 (2013).

34. Pursell, C. J., Chandler, B. D., Manzoli, M. & Boccuzzi, F. CO adsorption on supported gold nanoparticle catalysts: application of the temkin model. *J. Phy. Chem. C* 116, 11117–11125 (2012).

35. Kudo, S., Maki, T., Yamada, M. & Mae, K. A new preparation method of Au/ferric oxide catalyst for low temperature CO oxidation. *Chem. Eng. Sci.* 65, 214–219 (2010).

36. Jimenez-Lam, S. A. *et al.* Role of iron carbonyls in the inhibition of oxygen activation for the oxidation of CO catalyzed by iron oxide-supported gold. *Chem. Phys. Chem.* 13, 4173–4179 (2012).

37. Ojeda, M., Zhan, B.-Z. & Iglesia, E. Mechanistic interpretation of CO oxidation turnover rates on supported Au clusters. *J. Catal.* 285, 92–102 (2012).

38. Bond, G. C., Louis, C. & Thompson, D. T. In *Catalytic Science Series* Vol. 6, (ed Hutchings, G. J.) 176 (Imperial College Press, Singapore, 2006).

39. Lee, S. J. & Gavriilidis, A. Supported Au catalysts for low-temperature CO oxidation prepared by impregnation. *J. Catal.* 211, 283–283 (2002).

40. Jiao, F. *et al.* Ordered mesoporous Fe$_2$O$_3$ with crystalline walls. *J. Am. Chem. Soc.* 128, 5468–5474 (2006).

41. Wang, G., Lian, A., Zhang, W., Jiang, D. & Wu, T. Stability and deactivation of Au/Fe$_2$O$_3$ catalysts for CO oxidation at ambient temperature and moisture. *Kinet. Catal.* 43, 468–478 (2002).

42. Dormann, J. L., Cui, J. R. & Sella, C. Mossbauer studies of Fe$_2$O$_3$ antiferromagnetic small particles. *J. Appl. Phys.* 57, 4283–4285 (1985).

43. Zysler, R. D. *et al.* Size dependence of the spin-flop transition in hematite nanoparticles. *Phys. Rev. B: Condens. Matter* 68, 1–4 (2003).

44. Feng, C. *et al.* Ruthenium-catalyzed tertiary amine formation from nitroarenes and alcohols. *Org. Lett.* 12, 4888–4891 (2010).

45. Cui, X., Zhang, Y., Shi, F. & Deng, Y. Ruthenium-catalyzed nitro and nitrile compounds coupling with alcohols: alternative route for N-substituted amine synthesis. *Chem. Eur. J.* 17, 2587–2591 (2011).

Acknowledgments

Author contributions

F.S. and Y.D. supervised the project. C.Z., L.L. and X.C. performed the catalyst preparation and catalytic reactions. L.Z. performed the EXAFS analysis. C.Z., F.S. and Y.D. analysed the data and wrote the manuscript.

Additional information

Supplementary information accompanies this paper at http://www.nature.com/scientificreports

Competing financial interests: The authors declare no competing financial interests.

How to cite this article: Zhang, C.M. *et al.* Chlorine as an Indicator in the Controllable Preparation of Active Nano-Gold Catalyst. *Sci. Rep.* 3, 1503; DOI:10.1038/srep01503 (2013).